Eur. Phys. J. C 55, 249–258 (2008)
DOI 10.1140/epjc/s10052-008-0591-9

THE EUROPEAN
PHYSICAL JOURNAL C

Regular Article – Theoretical Physics

Contribution of the DK continuum in the QCD sum rule for $D_{sJ}(2317)$

Yuan-Ben Dai[1,a], Xin-Qiang Li[1,b], Shi-Lin Zhu[2,c], Ya-Bing Zuo[3,d]

[1] Institute of Theoretical Physics, Chinese Academy of Sciences, P.O. Box 2735, Beijing 100080, P.R. China
[2] Department of Physics, Peking University, Beijing 100871, P.R. China
[3] Department of Physics, Graduate School of Chinese Academy of Sciences, Beijing, P.R. China

Received: 11 February 2007 / Revised version: 27 October 2007 /
Published online: 24 April 2008 –

Abstract. Using the soft-pion theorem and the assumption on the final-state interactions, we include the contribution of the DK continuum into the QCD sum rules for the $D_{sJ}(2317)$ meson. We find that this contribution can significantly lower the mass and the decay constant of the $D_s(0^+)$ state. For the value of the current quark mass $m_c(m_c) = 1.286$ GeV, we obtain the mass of $D_s(0^+)$ $M = 2.33 \pm 0.02$ GeV in the interval $s_0 = 7.5$–$8.0\ \text{GeV}^2$, being in agreement with the experimental data, and the vector current decay constant of $D_s(0^+)$ $f_0 = 0.128 \pm 0.013$ GeV, much lower than those obtained in the previous literature.

PACS. 12.39.Hg; 13.25.Hw; 13.25.Ft; 12.38.Lg

1 Introduction

In 2003 the BaBar Collaboration discovered a positive-parity scalar charm strange meson $D_{sJ}(2317)$ with a very narrow width [1], which was confirmed by CLEO [2] later. In the same experiment CLEO also observed the 1^+ partner state at 2460 MeV [2]. Since these two states lie below the DK and D^*K threshold, respectively, the potentially dominant s-wave decay modes $D_{sJ}(2317) \to DK$ etc., are kinematically forbidden. Thus the radiative decays and isospin-violating strong decays become the dominant decay modes. Therefore both of them are very narrow.

The discovery of these two states has triggered a heated discussion on their nature in literature. The key point is to understand their low masses. The mass of $D_{sJ}(2317)$ is significantly lower than the expected values in the range of 2.4–2.6 GeV within quark models [3–5]. The model using the heavy-quark mass expansion of the relativistic Bethe–Salpeter equation predicted a lower value, 2.369 GeV [6], which is still higher than the experimental data by about 50 MeV.

Based on experience with $a_0/f_0(980)$, van Beveren and Rupp [7, 8] argued that the low mass of $D_{sJ}(2317)$ could arise from the mixing between the 0^+ $\bar{c}s$ state and the DK continuum. In this way the lowest 0^+ state could be pushed much lower than that expected from the quark models.

[a] e-mail: dyb@itp.ac.cn
[b] e-mail: xqli@itp.ac.cn
[c] e-mail: zhusl@phy.pku.edu.cn
[d] e-mail: yabingzuo@gucas.ac.cn

The mass of the $D_s(0^+)$ state from the lattice QCD calculation is also significantly larger than the experimentally observed mass of $D_{sJ}(2317)$ [9–11]. It is also pointed out in [9] that $D_{sJ}(2317)$ might receive a large component of the DK continuum, which makes the lattice simulation very difficult.

The difficulty with the $\bar{c}s$ interpretation leads many authors to speculate that $D_{sJ}(2317)$ is a $\bar{c}qs\bar{q}$ four-quark state [12, 13], or a strong $D\pi$ atom [14]. However, calculations based on the quark model show that the mass of the four-quark state is much larger than that of the 0^+ $\bar{c}s$ state [15, 16]. The radiative decay of $D_{sJ}(2317)$ also favors that it is a $\bar{c}s$ state [17]. Furthermore, there are two 0^+ states in the four-quark system and one in the two-quark system. Only one 0^+ state has been found below the 2.86 GeV resonance in the experimental search by BaBar [18], consistent with the $\bar{c}s$ interpretation.

This problem has been treated with QCD sum rules in the heavy-quark effective theory in [19]. The resulting $D_s(0^+)$ mass is consistent with the experimental data within large theoretical uncertainties. However, the central value is still larger than the data by 90 MeV. An even larger result for the $D_s(0^+)$ mass was obtained in earlier work with the sum rule in full QCD [20]. It has been pointed out in [19] that, in the formalism of QCD sum rules, the physics of mixing with the DK continuum resides in the contribution of the DK continuum in the sum rule, and including this characteristic contribution should render the mass of $D_s(0^+)$ lower.

Recently, there have been two investigations on this problem using sum rules in full QCD including $O(\alpha_s)$ corrections. In [21] the value of the charm quark pole mass $M_c = 1.46\,\text{GeV}$ is used, and the mass of the 0^+ $\bar{c}s$ state is found to be 100–200 MeV higher than the experimental data. On the other hand, in [22] the current quark mass $m_c = 1.15\,\text{GeV}$ (corresponding to $M_c \simeq 1.3\,\text{GeV}$ to $O(\alpha_s)$) is used, and the central value of the resulting 0^+ $\bar{c}s$ mass is in agreement with the data. However, a low value of m_c is used and the same value of the continuum threshold (denoted by s_0 below) is used for 0^+ $\bar{c}s$ and 0^- $\bar{c}s$.

On the other hand, the perturbative three-loop order α_s^2 correction to the two-point correlation function with one heavy and one massless quark has been calculated [23, 24]. It turns out that in the pole mass scheme used by many previous analyses including [21, 22], the perturbative expansion is far from converging. However, taking the quark mass in the modified minimal subtraction ($\overline{\text{MS}}$) scheme [25], better convergence of the higher order corrections is obtained, and thus a more reliable determination of physical quantities of the lowest lying resonances becomes feasible [26].

Usually the contribution of the two-particle continuum is neglected within the QCD sum rule formalism. However, because of the large s-wave coupling of $D_s(0^+)DK$ [27, 28] and the adjacency of the $D_s(0^+)$ mass to the DK threshold, this contribution may not be neglected in the case considered. In the present work, we shall therefore calculate this contribution and include it in the QCD sum rule. In the meantime we take into account the perturbative three-loop order α_s^2 correction and work in the $\overline{\text{MS}}$ scheme. We find that the DK continuum contribution indeed renders both the mass and the decay constant of $D_s(0^+)$ significantly lower.

In Sect. 2, we give a short overview of the traditional QCD sum rule for the scalar charm-strange meson. Then we derive the DK continuum contribution and write down the full sum rule in Sect. 3. Finally, the numerical results and our conclusions are presented in Sect. 4. Some relevant formulas and expressions used in this paper are collected in Appendices A–C.

2 The traditional QCD sum rule for the scalar charm-strange meson

We consider the scalar correlation function

$$\Pi(p^2) \equiv \mathrm{i} \int \mathrm{d}x \mathrm{e}^{\mathrm{i}px} \langle 0| T\{j(x) j(0)^\dagger\}|\, 0\rangle\,, \qquad (1)$$

where the renormalization invariant operator $j(x)$ is defined as

$$j(x) = (m_c - m_s) : \bar{s}(x) c(x) :\,, \qquad (2)$$

with m_c and m_s being the charm and strange quark current mass, respectively. Up to a subtraction polynomial in p^2, the correlation function $\Pi(p^2)$ satisfies the following dispersion relation:

$$\Pi(p^2) = \int_0^\infty \frac{\rho(s)}{(s - p^2 - \mathrm{i}\epsilon)}\, \mathrm{d}s + \text{subtractions}\,. \qquad (3)$$

At the quark–gluon level, the spectral function $\rho(s)$ is calculable using renormalization group improved perturbation theory in the framework of the operator product expansion (OPE). Following Jamin and Lange [26], in this paper we shall adopt the $\overline{\text{MS}}$ running quark mass scheme rather than the pole mass one and take into account both the $O(\alpha_s^2)$ terms in the perturbation theory obtained in [23, 24] and the corrections from the light quark mass up to order m_s^4. In addition, we have included the contribution from the four-quark condensation, which affects the final result for $D_s(0^+)$ mass only by a few MeV. For convenience, all the relevant expressions for $\rho(s)$ at the quark–gluon level, denoted by $\rho_{\text{QCD}}(s)$, are summarized in Appendix A. On the other hand, $\rho(s)$ can be phenomenologically written in terms of contributions from intermediate hadronic states. Generally, the spectral density at the hadronic level, denoted by ρ_{H}, is taken to be the pole term of the lowest lying hadronic state plus the continuum starting from some threshold, with the latter identified with the QCD continuum,

$$\frac{\rho_{\text{H}}(t)}{\pi} = f_0^2 M^4 \delta(t - M^2) + \textbf{QCD continuum} \times \theta(t - s_0)\,, \qquad (4)$$

where f_0 is the vector current decay constant of the 0^+ $\bar{c}s$ particle, analogous to $f_\pi = 131\,\text{MeV}$. M is the mass of this particle, and s_0 is the continuum threshold above which the hadronic spectral density is modeled by that at the quark–gluon level. The recent works [21, 22] also use the above ansatz.

After making the Borel transformation to suppress the contribution of the higher excited states and invoking quark–hadron duality, one arrives at the sum rule

$$\int \mathrm{d}t \frac{\rho_{\text{H}}(t)}{\pi} \exp\left[-\frac{t}{M_{\text{B}}^2}\right] = \int_{M_c^2}^\infty \mathrm{d}t \frac{\rho_{\text{QCD}}(t)}{\pi} \exp\left[-\frac{t}{M_{\text{B}}^2}\right]. \qquad (5)$$

Following [26], the lower limit of the integration in the above equation is taken to be the charm quark pole mass M_c, which can be expressed in terms of the running mass $m_c(\mu_m)$ through the perturbative three-loop relation as defined in Appendix B.

3 The contribution of the DK continuum

The contribution of two-particle continuum to the spectral density can safely be neglected in many cases, as usually is done in the traditional QCD sum rule analysis. One typical example is the ρ meson sum rule, where the two pion continuum is of p-wave nature. Its contribution to the spectral density is tiny and the ρ pole contribution dominates.

However, there may be an exception when the 0^+ particle couples strongly to the two-particle continuum via the s-wave. In such a case, there is no threshold suppression and the two-particle continuum contribution may be more significant. The strong coupling of the 0^+ particle with the two-particle state and the adjacency of the 0^+ mass to the DK continuum threshold result in a large coupling channel effect, which corresponds to the configuration of mixing in the formalism of quark model. In the problem under consideration, the mass of $D_{sJ}(2317)$ is only about 45 MeV below the DK threshold, and the s-wave coupling of $D_s(0^+)DK$ is found to be very large [27, 28]. Therefore, one may have to take into account the DK continuum contribution carefully.

The importance of the $D\pi$ continuum contribution in the sum rule for the $D(0^+)$ meson was first emphasized in [29], based on duality considerations in the case in which the $D(0^+)$ mass is higher than the $D\pi$ threshold. Based on the soft-pion theorem, two of us also made a crude analysis of the $B\pi$ continuum contribution in the case in which the 0^+ particle mass is higher than the threshold [28]. In this work, we calculate the continuum contribution more carefully in the case in which the 0^+ particle mass is lower and very close to the two-particle continuum threshold.

Let $F(t)$ be the form-factor defined by

$$F(t) = \langle 0|\bar{c}(0)s(0)|DK\rangle \,. \tag{6}$$

From the large s-wave coupling of $D_s(0^+)DK$ and the adjacency of the $D_s(0^+)$ mass to the DK threshold, one expects that in the low energy region $F(t)$ is dominated by the product of a factor of the $D_s(0^+)$ pole and a factor from the final-state interactions. In the low energy region with $(m_D+m_K)^2 < t < s_0 \leq 8\,\mathrm{GeV}^2$, needed in our sum rule, the effect of inelastic DK scattering is suppressed by the phase space. Therefore, we take the approximation of considering only the DK scattering with only elastic intermediate states. It can be described by the $D_s(0^+)DK$ interaction and the $DDKK$ chiral interaction in the low energy effective Lagrangian, which can be represented by a series of bubble diagrams shown in Fig. 1.

The s-wave Born amplitude of DK scattering represented by the black circles in Fig. 1 contains three terms. The first one is the t channel pole term $\frac{-\mathrm{i}g_0^2}{t-M_0^2}$, with g_0 being the $D_s(0^+)DK$ coupling constant and M_0 being the mass parameter normalized at the scale m_D^2 in the effective Lagrangian.

The second term corresponds to the direct $DDKK$ interaction in the effective Lagrangian. Let p, k and p', k' be the four-momentum of the D and K mesons in the initial and final state respectively, and $s=(p-k')^2=(p'-k)^2$. In the chiral effective Lagrangian, the amplitudes for the processes $D^+K^0 \to D^+K^0$, $D^0K^+ \to D^0K^+$, and $D^+K^0 \leftrightarrow D^0K^+$ in the low energy k_0 region of K meson needed in the QCD sum rule are all equal to

$$\frac{\mathrm{i}}{2}\int_{-1}^{+1}\mathrm{d}\cos\theta\frac{t-s}{2f_K^2} = \frac{\mathrm{i}}{2f_K^2}\left[2\sqrt{t}(k_0+k_0')-2k_0k_0'-k^2-k'^2\right], \tag{7}$$

in the center of mass system. Here k and k' should be separately included in the integrals for two adjacent loops.

The third term of the s-wave Born amplitude arises from the crossing s channel pole term

$$-\mathrm{i}\frac{g_0^2}{2}\int_{-1}^{+1}\mathrm{d}\cos\theta\,\frac{1}{s-M_0^2} = \mathrm{i}\frac{g_0^2}{2}\frac{1}{B}\ln\frac{A-B}{A+B}\,, \tag{8}$$

where

$$A = t-2\sqrt{t}(k_0+k_0')+2k_0k_0'+2m_K^2-M_0^2, \quad B=2|\mathbf{k}|\,|\mathbf{k}'|. \tag{9}$$

For simplicity, we put the on-shell values of k_0, k_0', $|\mathbf{k}|$ and $|\mathbf{k}'|$ into A and B in the above equations. The effect of this approximation on our final results is expected to be small, since the contribution of the s channel pole term is relatively small. As a result, one finds that the s channel pole term is an analytic function of t with only a short cut, the length of which is only $0.146\,\mathrm{GeV}^2$ for experimental values of the corresponding masses. Therefore, it can be well approximated by a pole form $-\mathrm{i}\frac{cg_0^2}{t-t_0}$, where

$$t_0 = \frac{1}{2}\left[2m_D^2+2m_K^2-M_0^2+\frac{(m_D^2-m_K^2)^2}{M_0^2}\right], \tag{10}$$

$$c = \frac{2m_D^2+2m_K^2-M_0^2-\frac{(m_D^2-m_K^2)^2}{M_0^2}}{\frac{(m_D^2-m_K^2)^2}{t_0}+t_0-2m_D^2-2m_K^2}\,. \tag{11}$$

With the above results for the three terms of the s-wave Born amplitude, we can now evaluate the sum of the series of the bubble diagrams shown in Fig. 1. Let $f_n(t)$ be the partial sum of the series of loop diagrams in Fig. 1, with the loop number less than or equal to n. It can then be written in the form

$$f_n(t) = \frac{-1}{2f_K^2}\left\{\left[\left(2\sqrt{t}k_0'-k'^2\right)-2f_K^2\left(\frac{g_0^2}{t-M_0^2}+\frac{cg_0^2}{t-t_0}\right)\right]f_{n0} + 2\left(\sqrt{t}-k_0'\right)f_{n1}-f_{n2}\right\}, \tag{12}$$

where k_0' and k' is the energy and momentum of the final-state K meson, and the three unknown functions f_{ni} ($i=0,1,2$) correspond to the diagrams with a factor 1, k_0, and k^2 respectively at the last vertex, which contributes to the integration over the last loop of each diagram.

Let the $\Sigma_i(t)$ be integrals defined by (C.1)–(C.6), which appear as the loop integrals of the individual loop diagrams shown in Fig. 1. They can be evaluated using dimensional regularization [30], with the corresponding analytic results given in (C.1)–(C.6). A recurrence relation can be written between $f_n(t)$ and $f_{(n+1)}(t)$, and hence between $f_{ni}(t)$

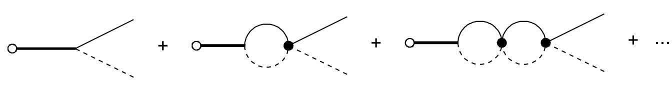

Fig. 1. *Heavy*, *light*, and *dotted lines* represent $D_s(0^+)$, D, and K, respectively. The *black circle* represents the Born s-wave amplitude of DK scattering, and the *blank one* the scalar current

and $f_{(n+1)i}(t)$, the coefficients of which are linear combinations of the loop-integral functions $\Sigma_i(t)$. Taking the limit $\lim_{n\to\infty} f_{ni}(t) = f_i(t)$, $\lim_{n\to\infty} f_n(t) = f(t)$, and separating out terms with the factor 1, k'_0 and k'^2, we can obtain a system of three linear equations for the three unknown functions $f_i(t)$:

$$
\begin{aligned}
&2f_1\Sigma_4 + f_0\Sigma_5 - 2[f_1(2\Sigma_2+\Sigma_3)+2f_0\Sigma_4]\sqrt{t} \\
&+4(f_1\Sigma_1+f_0\Sigma_2)t + 4f_K^4 g_0^2\left[g_0\Sigma_0 - f_0\left(M_0^2+g_0^2\Sigma_0-t\right)\right] \\
&\times\left[\frac{c}{(t-t_0)^2}+\frac{1}{\left(t-M_0^2\right)(t-t_0)}\right] \\
&+2f_K^2\Big\{g_0(1-2f_0g_0)\left(2\Sigma_1\sqrt{t}-\Sigma_3\right) \\
&\quad +2f_1\left[g_0^2\Sigma_1-\left(M_0^2+g_0^2\Sigma_0\right)\sqrt{t}+t^{\frac{3}{2}}\right]\Big\}\frac{1}{t-M_0^2} \\
&+f_2\left[\Sigma_3-2\Sigma_1\sqrt{t}+2f_K^2g_0^2\Sigma_0\left(\frac{1}{t-M_0^2}+\frac{c}{t-t_0}\right)-2f_K^2\right] \\
&+2f_K^2\frac{2cg_0^2\left[f_1\Sigma_1+f_0\Sigma_3-(f_1\Sigma_0+2f_0\Sigma_1)\sqrt{t}\right]}{t-t_0} \\
&+4cf_0f_K^4g_0^4\Sigma_0\left[\frac{c}{(t-t_0)^2}+\frac{1}{\left(t-M_0^2\right)(t-t_0)}\right]=0\,, \qquad (13)
\end{aligned}
$$

$$
\begin{aligned}
&f_2\Sigma_1+f_0\Sigma_4-[f_2\Sigma_0+f_0(2\Sigma_2+\Sigma_3)]\sqrt{t} \\
&+2f_1\left(-f_K^2+\Sigma_2-2\Sigma_1\sqrt{t}+\Sigma_0 t\right) \\
&+2f_K^2\frac{g_0(1-f_0g_0)\Sigma_1+\left[f_0M_0^2-g_0(1-f_0g_0)\Sigma_0\right]\sqrt{t}-f_0t^{\frac{3}{2}}}{M_0^2-t} \\
&+2f_0\Sigma_1 t+2f_K^2\frac{cf_0g_0^2\left(\Sigma_1-\Sigma_0\sqrt{t}\right)}{t-t_0}=0\,, \qquad (14)
\end{aligned}
$$

$$
\begin{aligned}
&2f_1\Sigma_1+f_0\left[\Sigma_3-2\Sigma_1\sqrt{t}+2f_K^2g_0^2\Sigma_0\left(\frac{1}{t-M_0^2}+\frac{c}{t-t_0}\right)\right. \\
&\left.-2f_K^2\right]+\Sigma_0\left(f_2-\frac{2f_K^2g_0}{t-M_0^2}-2f_1\sqrt{t}\right)=0\,, \qquad (15)
\end{aligned}
$$

from which the analytic forms for $f_i(t)$ can then be deduced. The results are shown in (C.9)–(C.12).

Finally, with the explicit expressions for $f_i(t)$ and $\Sigma_i(t)$ given in Appendix C, and putting the on-shell value of k' to (12), we obtain

$$
\begin{aligned}
F(t) &= \frac{-g_0}{t-M_0^2}-\frac{1}{2f_K^2}\Big\{\Big[\left(t-m_D^2\right) \\
&\quad -2f_K^2\left(\frac{g_0^2}{t-M_0^2}+\frac{cg_0^2}{t-t_0}\right)\Big]f_0+\frac{t+m_D^2-m_K^2}{\sqrt{t}}f_1-f_2\Big\} \\
&= \frac{\lambda}{t-M_0^2-\Delta(t)}\,, \qquad (16)
\end{aligned}
$$

where $\Delta(t)$ is given by (C.13).

Similarly, with the same series of DK loops included, the full propagator of the $D_s(0^+)$ meson is related to the function $f_0(t)$ through

$$
\mathrm{Prop}(t) = \frac{\mathrm{i}}{t-M_0^2}[1-g_0f_0(t)]\,. \qquad (17)
$$

Using the solution for $f_0(t)$ obtained above and given by (C.9), it can be further rewritten as

$$
\mathrm{Prop}(t) = \frac{1}{t-M_0^2-\Delta_1(t)}\,, \qquad (18)
$$

with $\Delta_1(t)$ given by (C.14).

We have chosen the scale μ so that the mass parameter M_0 is the physical mass of $D_s(0^+)$ in our approximation, i.e., $\Delta_1(M_0^2)=0$. The bare coupling constant g_0 is related to the physical coupling constant g by $g=g_0/\sqrt{Z}$, where

$$
Z = \frac{\mathrm{d}}{\mathrm{d}t}\left[t-M_0^2-\Sigma(t)\right]_{t=M_0^2}\,, \qquad (19)
$$

is the on-shell wave function renormalization constant of the $D_s(0^+)$ meson.

In order to fix the unknown constant λ in $F(t)$ given by (16), we apply the soft-pion theorem

$$
F\left(m_D^2\right) = \frac{f_Dm_D^2}{f_K(m_c+m_u)} \qquad (20)
$$

to the extrapolated value of the matrix element $\langle 0|\bar{c}(0)s(0)|DK\rangle$ at $t=m_D^2$, from which we can deduce the constant:

$$
\lambda = \frac{f_Dm_D^2}{f_K(m_c+m_u)}\left[M_D^2-M_0^2-\Delta\left(m_D^2\right)\right]. \qquad (21)
$$

With all the above equipments, the DK continuum contribution to the hadronic spectral function can then be written as

$$
\begin{aligned}
\rho_{DK}(t) &= \frac{1}{8\pi^2}\sqrt{1-\frac{(m_D+m_K)^2}{t}}\sqrt{1-\frac{(m_D-m_K)^2}{t}} \\
&\quad\times(m_c-m_s)^2|F(t)|^2\theta\left(\sqrt{t}-m_D-m_K\right)\theta(s_0-t)\,. \qquad (22)
\end{aligned}
$$

In the above calculations we have neglected the contribution of the $D_s\eta$ channel. The threshold of this channel is at $t=6.329\,\mathrm{GeV}^2$. Our formula for the contribution of the two-particle term is proportional to $(t-M_0^2)^{-2}$. The lower part of the integration in t is more important. At the thresholds of the two channels the factor $(t-M_0^2)^{-2}$ for the DK channel is about 18 times larger than that for the $D_s\eta$ channel. Therefore, the effect of the latter is expected to be small.

4 Numerical results and discussions

In our numerical analysis, we use the recent result for the c quark current mass $m_c(m_c)=1.286\,\mathrm{GeV}$ [31]. Other input parameters are the following (assuming the isospin symmetry): $\alpha_s(m_Z)=0.1189$ [32], $m_s(2\,\mathrm{GeV})=96.10\,\mathrm{MeV}$ [33], $m_u(2\,\mathrm{GeV}) = m_s(2\,\mathrm{GeV})/24.4$ [33], $\langle\bar{s}s\rangle = 0.8\times(-0.243)^3\,\mathrm{GeV}^3$ [22], $\langle\bar{s}g_s\sigma\cdot Gs\rangle = 0.8\,\mathrm{GeV}^2\times\langle\bar{s}s\rangle$ [22], $\langle\alpha_sG^2\rangle = 0.06\,\mathrm{GeV}^4$ [22], in the four-quark condensation term (A.15) $\sigma=3$, $m_D=\frac{m_{D^\pm}+m_{D^0}}{2}=1866.9\,\mathrm{MeV}$ [34],

$m_K = \frac{m_{K^\pm}+m_{K^0}}{2} = 495.66\,\text{MeV}$ [34], $f_D = 222.6\,\text{MeV}$ [34] and $f_K = 159.8\,\text{MeV}$ [34].

The renormalized coupling constant g was determined to be in the interval $g = 5.1$–$7.5\,\text{GeV}$ in [27, 28]. Inclusion of the contribution of the DK continuum in the sum rule analysis of the scalar current channel will lower the g value. Since the uncertainty is large, we have not calculated this correction and simply allow the renormalized g to vary in the region $g = 4.0$–$7.0\,\text{GeV}$.

A resonance of the D_s system with the natural parity has been observed experimentally at $t = 8.18\,\text{GeV}^2$ [18]. If it is an excited state of $D_s(0^+)$, we should restrict ourselves to s_0 smaller than and close to $8.0\,\text{GeV}^2$. We shall first consider this case and then discuss the case that this resonance is not a 0^+ state. The convergence of the OPE series and dominance of the sum by the pole and the DK continuum terms over the QCD continuum beyond s_0 constrain the Borel mass M_B in a region depending on the parameters $m_c(m_c)$ and s_0. Taking $m_c = 1.286\,\text{GeV}$, $M_\text{B}^2 \in [0.99, 2.68]\,\text{GeV}^2$ for $s_0 = 8.0\,\text{GeV}^2$, and $M_\text{B}^2 \in [0.99, 2.41]\,\text{GeV}^2$ for $s_0 = 7.5\,\text{GeV}^2$. As mentioned in [26, 35, 36], the convergence of the perturbative expansion of the two-point correlation function, when written in terms of the pole quark mass, is rather poor, the order α_s and α_s^2 loop contributions being of similar size with, or even larger than, the leading term, while the expansion in terms of the $\overline{\text{MS}}$ running mass converges much faster. However, it should be noted that, even in the $\overline{\text{MS}}$ running mass scheme, the convergence of the asymptotic series in the D_s meson system is worse than the one found in the B_s meson system. For $D_s(0^+)$ the first order correction amounts to about 53% and the second order correction to about 47% of the leading term using the values of our input parameters and $s_0 = 8.0\,\text{GeV}^2$. The same observation has also been made in [35].

We first move the DK continuum contribution to the right hand side of the sum rule. Then we obtain the curve of M with respect to M_B by taking the derivative of the logarithm of both sides of the sum rule as usually done. Since this curve depends on the unknown parameters M_0, we have to do it self-consistently by requiring that the M value determined by the sum rule for the input "trial" value of M_0 lies in the middle of the stability window and roughly equals M_0. For reliability of the results we also require that the ratio of DK contribution to the whole sum rule is not larger than about 60%.

With the input $m_c(m_c) = 1.286\,\text{GeV}$, we present the variation of M with M_B^2 for $s_0 = 8.0\,\text{GeV}^2$ and $s_0 = 7.5\,\text{GeV}^2$ in Figs. 2 and 3, respectively. For comparison, we also show the case without the DK continuum contribution with the same set of input parameters. It can be seen clearly from the two figures that the inclusion of the DK continuum contribution can lower the M value by 60–40 MeV. The DK continuum contributes around 45% to 60% of the right hand side of the final sum rule for $s_0 = 8.0\,\text{GeV}^2$ as shown in Fig. 4. Another interesting point concerns the vector current decay constant f_0 of the $D_s(0^+)$ meson. We find that the inclusion of the DK continuum contribution lowers the decay constant f_0 from about 0.185 GeV to 0.115–0.132 GeV for the same s_0 value as can be seen from Fig. 5.

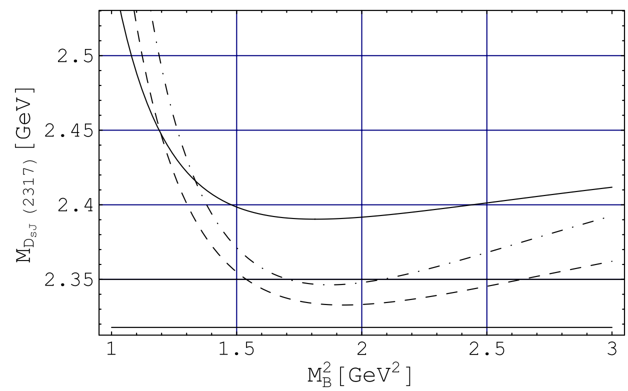

Fig. 2. The variation of M with M_B^2 when $s_0 = 8.0\,\text{GeV}^2$. The *solid*, *dashdotted*, and *dashed curves* are for the case without the DK continuum contribution, $g = 4.0$ GeV, and $g = 7.0$ GeV, respectively

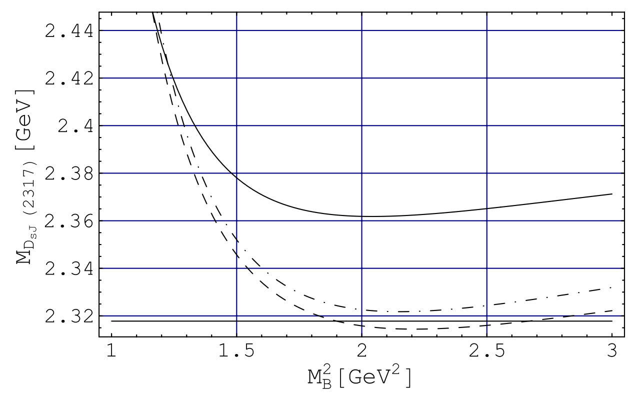

Fig. 3. The variation of M with M_B^2 when $s_0 = 7.5\,\text{GeV}^2$. The other captions are the same as in Fig. 2

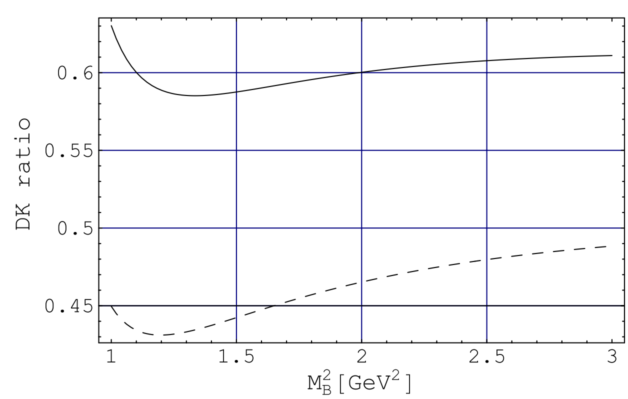

Fig. 4. The ratio of the DK continuum contribution as a function of M_B^2 with $s_0 = 8.0\,\text{GeV}^2$. The *solid* and *dashed curves* are for $g = 4.0$ GeV, and $g = 7.0$ GeV, respectively

For $m_c(m_c) = 1.286\,\text{GeV}$ and $s_0 = 7.5$–$8.0\,\text{GeV}^2$, we found $M = 2.331 \pm 0.016\,\text{GeV}$, in agreement with the experimental data $2317.8 \pm 0.6\,\text{MeV}$ [34]. For the same value of input parameters, we found $f_0 = 0.128 \pm 0.013\,\text{GeV}$, which is, however, significantly lower than the ones obtained in the previous literature. Here we have not included

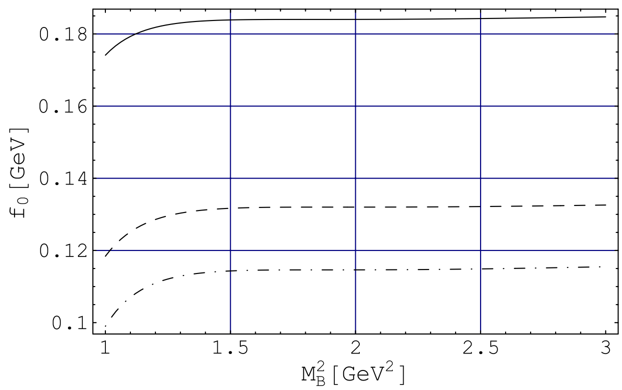

Fig. 5. The vector current decay constant f_0 as a function of M_{B}^2 with $s_0 = 8.0\,\mathrm{GeV}^2$. The other captions are the same as in Fig. 2

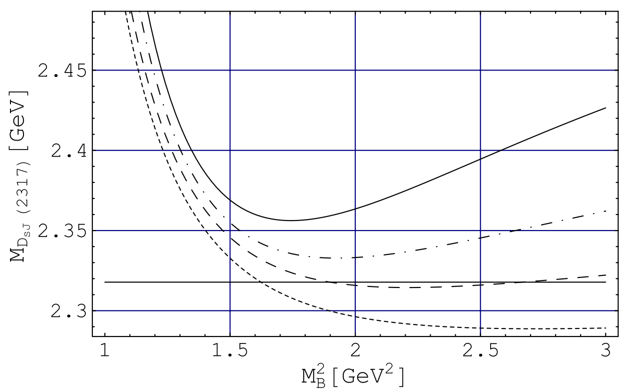

Fig. 6. The variation of M with M_{B}^2 when $g = 7\,\mathrm{GeV}^2$. The *solid*, *dashdotted*, *dashed* and *dotted curves* are for the case $s_0 = 8.5$, 8.0, 7.5, and $7.0\,\mathrm{GeV}^2$ respectively

the errors due to uncertainties in the QCD sum rule except those from the variation of the results in the stability window and the s_0 interval, since our main interest is the central value of the results. The previous results already showed that the $D_s(0^+)$ mass lies in the large uncertainty interval of the QCD sum rule [21, 22].

Now we consider the case that the new resonance found in [18] is not a 0^+ state. In this case the s_0 value can only be determined by a stability analysis. The results for the mass M found for $s_0 = 8.5, 8.0, 7.5, 7.0\,\mathrm{GeV}^2$ for $g = 7\,\mathrm{GeV}$ and $g = 4\,\mathrm{GeV}$ are shown in Figs. 6 and 7, respectively. The working region for $s_0 = 8.5\,\mathrm{GeV}^2$ and $s_0 = 7.0\,\mathrm{GeV}^2$ are $[0.99, 2.96]\,\mathrm{GeV}^2$ and $[0.99, 2.13]\,\mathrm{GeV}^2$, respectively. The region of the s_0 value can be chosen by requiring the least sensitivity of the results for the mass to the value of s_0. It is clear from these figures that this is the region between $s_0 = 7.5\,\mathrm{GeV}^2$ and $s_0 = 8.0\,\mathrm{GeV}^2$, which is just the region chosen above for the case of a 0^+ resonance at $t = 8.18\,\mathrm{GeV}^2$. Also the best stability with respect to M_{B} is achieved at $s_0 = 7.5\,\mathrm{GeV}^2$. Therefore, the results obtained above are essentially unchanged.

The above results show that the contribution of the DK continuum, which contains the physics of the coupled channel effect in the formalism of the QCD sum rule, is significant and is partly the reason for the unexpected low mass of the 0^+ $\bar{c}s$ state. Our analysis also explains partly why the extracted mass of the 0^+ $\bar{c}s$ state from the quenched lattice QCD simulation is higher than the experimental value where the DK continuum contribution was not included.

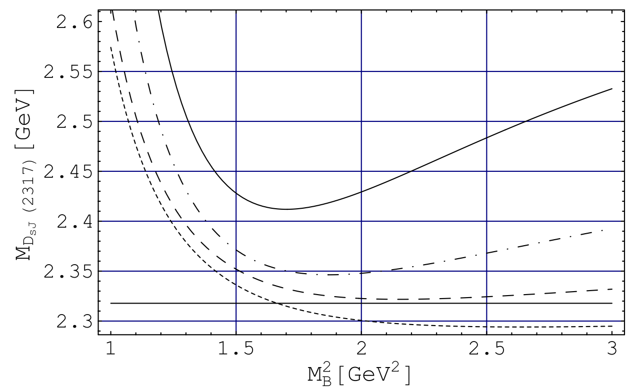

Fig. 7. The variation of M with M_{B}^2 when $g = 4\,\mathrm{GeV}^2$. The *solid*, *dashdotted*, *dashed* and *dotted curves* are for the case $s_0 = 8.5$, 8.0, 7.5, and $7.0\,\mathrm{GeV}^2$ respectively

Acknowledgements. We thank Prof. H.-Y. Cheng for beneficial discussion and Dr. Chun Liu and Dr. Xiang Liu for their kind help. S.L.Z. was supported by the National Natural Science Foundation of China under Grants No. 10625521 and No. 10721063 and Ministry of Education of China.

Appendix A: The spectral function $\rho_{\mathrm{QCD}}(s)$ at the quark–gluon level

In this appendix, all the relevant expressions for the spectral function $\rho(s)$ are given. For further details, we refer the readers to [26] and references therein.

A.1 The perturbative spectral function

In perturbation theory, the spectral function $\rho_{\mathrm{QCD}}(s)$ has an expansion in powers of the strong coupling constant

$$\rho_{\mathrm{QCD}}(s) = \rho^{(0)}(s) + \rho^{(1)}(s)a(\mu_a) + \rho^{(2)}(s)a(\mu_a)^2 + \dots\,, \tag{A.1}$$

with $a(\mu_a) \equiv \alpha_{\mathrm{s}}(\mu_a)/\pi$. The leading order term $\rho^{(0)}(s)$ results from a calculation of the bare quark–antiquark loop and is given by

$$\rho^{(0)}(s) = \frac{N_c}{8\pi^2}(m_c + m_s)^2 s\left(1 - \frac{m_c^2}{s}\right)^2, \tag{A.2}$$

and, up to order m_s^4, the corrections in small mass m_s can be found in [37]:

$$\rho_m^{(0)}(s) = \frac{N_c}{8\pi^2}(m_c + m_s)^2\left\{2(1-x)m_c m_s - 2m_s^2 - 2\frac{(1+x)}{(1-x)}\frac{m_c m_s^3}{s} + \frac{(1-2x-x^2)}{(1-x)^2}\frac{m_s^4}{s}\right\}, \tag{A.3}$$

where $x \equiv m_c^2/s$, and the appearing quark masses correspond to the running masses in the $\overline{\mathrm{MS}}$ scheme with $m_c(\mu_m)$ and $m_s(\mu_m)$ evaluated at the scale μ_m.

The order α_s correction $\rho^{(1)}(s)$ can be written as

$$\begin{aligned}\rho^{(1)}(s) = &\frac{N_c}{16\pi^2} C_F (m_c+m_s)^2 s(1-x)\Big\{(1-x)\\ &\times[4L_2(x)+2\ln x\ln(1-x)-(5-2x)\ln(1-x)]\\ &+(1-2x)(3-x)\ln x+3(1-3x)\ln\frac{\mu_m^2}{m_c^2}\\ &+\frac{1}{2}(17-33x)\Big\},\end{aligned} \tag{A.4}$$

where $L_2(x)$ is the dilogarithmic function. The order α_s mass corrections to the spectral function can be obtained by expanding the results given by [38, 39] up to order m_s^4, after the higher dimensional operators have been expressed in terms of non-normal ordered condensates:

$$\begin{aligned}\rho_m^{(1)}(s) = &\frac{N_c}{8\pi^2} C_F (m_c+m_s)^2 m_c m_s\Big\{(1-x)\\ &\times[4L_2(x)+2\ln x\ln(1-x)-2(4-x)\ln(1-x)]\\ &+2(3-5x+x^2)\ln x+3(2-3x)\ln\frac{\mu_m^2}{m_c^2}\\ &+2(7-9x)\Big\},\end{aligned} \tag{A.5}$$

$$\begin{aligned}\rho_{m^2}^{(1)}(s) = &-\frac{N_c}{8\pi^2} C_F (m_c+m_s)^2 m_s^2\\ &\times\Big\{(1-x)[4L_2(x)+2\ln x\ln(1-x)]\\ &-(2+x)(4-x)\ln(1-x)+(6+2x-x^2)\ln x\\ &+6\ln\frac{\mu_m^2}{m_c^2}+(8-3x)\Big\},\end{aligned} \tag{A.6}$$

$$\begin{aligned}\rho_{m^3}^{(1)}(s) = &-\frac{N_c}{8\pi^2} C_F (m_c+m_s)^2 \frac{m_c m_s^3}{s}\\ &\times\Big\{4L_2(x)+2\ln x\ln(1-x)+\frac{(9+8x-9x^2)}{(1-x)^2}\\ &-2\frac{(7+7x-2x^2)}{(1-x)}\ln(1-x)+2\frac{(6+7x-2x^2)}{(1-x)}\ln x\\ &+6\frac{(2-x^2)}{(1-x)^2}\ln\frac{\mu_m^2}{m_c^2}\Big\},\end{aligned} \tag{A.7}$$

$$\begin{aligned}\rho_{m^4}^{(1)}(s) = &\frac{N_c}{8\pi^2} C_F (m_c+m_s)^2 \frac{m_s^4}{s}\Big\{2L_2(x)+\ln x\ln(1-x)\\ &-\frac{(13-24x-27x^2+2x^3)}{2(1-x)^2}\ln(1-x)\\ &+\frac{(12-22x-27x^2+2x^3)}{2(1-x)^2}\ln x\\ &+3\frac{(4-12x+x^2+3x^3)}{2(1-x)^3}\ln\frac{\mu_m^2}{m_c^2}\\ &+\frac{(6-64x+15x^2+11x^3)}{4(1-x)^3}\Big\}.\end{aligned} \tag{A.8}$$

The three-loop, order α_s^2 correction $\rho^{(2)}(s)$ has been calculated by Chetyrkin and Steinhauser [23, 24] for the case of one heavy and one massless quark. In the present analysis, we shall make use of the program Rvs.m, which contains the required expressions for $\rho^{(2)}(s)$ [23, 24]. However, since the spectral function has been calculated only in the pole mass scheme, following Jamin and Lange [26], in the $\overline{\mathrm{MS}}$ scheme we still have to add to $\rho^{(2)}(s)$ the contributions resulting from rewriting the pole mass in terms of the $\overline{\mathrm{MS}}$ mass. The two contributions $\Delta_1\rho^{(2)}$ and $\Delta_2\rho^{(2)}$, which arise from the leading and first order contributions, respectively, are given by

$$\begin{aligned}\Delta_1\rho^{(2)}(s) = &\frac{N_c}{8\pi^2}(m_c+m_s)^2 s\big[(3-20x+21x^2){r_m^{(1)}}^2\\ &-2(1-x)(1-3x)r_m^{(2)}\big],\end{aligned} \tag{A.9}$$

$$\begin{aligned}\Delta_2\rho^{(2)}(s) = &-\frac{N_c}{8\pi^2} C_F (m_c+m_s)^2 s r_m^{(1)}\\ &\times\Big\{(1-x)(1-3x)[4L_2(x)+2\ln x\ln(1-x)]\\ &-(1-x)(7-21x+8x^2)\ln(1-x)\\ &+(3-22x+29x^2-8x^3)\ln x\\ &+\frac{1}{2}(1-x)(15-31x)\Big\},\end{aligned} \tag{A.10}$$

where explicit expressions for the coefficients $r_m^{(1)}$ and $r_m^{(2)}$ can be found in Appendix B.

A.2 The condensate contributions

In the following, we summarize the contributions to the spectral function $\rho_{\mathrm{QCD}}(s)$ coming from higher dimensional operators, which arise in the framework of the OPE and parameterize the appearance of non-perturbative physics. Since the spectral functions corresponding to the condensates contain δ-distribution contributions, we shall directly present the Borel transformed integrated quantity $u\widehat{\Pi}(u) = \int_0^\infty \mathrm{e}^{-s/u}\rho_{\mathrm{QCD}}(s)\,\mathrm{d}s$ below, where $u = M_B^2$ with M_B being the Borel mass.

The leading order expression for the dimension-three quark condensate is well known, with the explicit form given by

$$\begin{aligned}u\widehat{\Pi}_{\bar{q}q}^{(0)}(u) = &-(m_c+m_s)^2 m_c\langle\bar{q}q\rangle \mathrm{e}^{-m_c^2/u}\\ &\times\left[1-\left(1+\frac{m_c^2}{u}\right)\frac{m_s}{2m_c}+\frac{m_c^2 m_s^2}{2u^2}\right],\end{aligned} \tag{A.11}$$

where the expansion up to order m_s^2 has been included [37]. The first order correction to the quark condensate can be deduced based on the fact that the mass logarithms must cancel once the quark condensate is expressed in terms of the non-normal ordered condensate [37, 40–42] with

$$\begin{aligned}u\widehat{\Pi}_{\bar{q}q}^{(1)}(u) = &\frac{3}{2} C_F a (m_c+m_s)^2 m_c\langle\bar{q}q\rangle\Big\{\Gamma\left(0,\frac{m_c^2}{u}\right)\\ &-\left[1+\left(1-\frac{m_c^2}{u}\right)\left(\ln\frac{\mu_m^2}{m_c^2}+\frac{4}{3}\right)\right]\mathrm{e}^{-m_c^2/u}\Big\},\end{aligned} \tag{A.12}$$

where $\Gamma(n,z)$ is the incomplete Γ-function.

The next contribution in the OPE is the dimension-four gluon condensate with the corresponding expression given by

$$u\widehat{\Pi}^{(0)}_{FF}(u)=\frac{1}{12}(m_c+m_s)^2\langle aFF\rangle \mathrm{e}^{-m_c^2/u}\,. \tag{A.13}$$

The dimension-five mixed quark–gluon condensate should also be included, since it is enhanced by the heavy-quark mass and hence still has some influence on the sum rule. Again the result is well known:

$$u\widehat{\Pi}^{(0)}_{\bar{q}Fq}(u)=-(m_c+m_s)^2\frac{m_c\langle g_s\bar{q}\sigma Fq\rangle}{2u}\left(1-\frac{m_c^2}{2u}\right)\mathrm{e}^{-m_c^2/u}\,. \tag{A.14}$$

The last condensate contribution considered in this paper is the four-quark condensate

$$u\widehat{\Pi}^{(0)}_{(\bar{s}s)^2}(u)=-\sigma\frac{8\pi}{27}\left(2-\frac{m_c^2}{2u}-\frac{m_c^4}{6u^2}\right)\alpha_s\langle\bar{s}s\rangle^2\,, \tag{A.15}$$

where σ is the factor representing the deviation from vacuum saturation. The contributions of all the other higher dimensional operators are extremely small and thus have been neglected.

Appendix B: Relationship between pole and running $\overline{\text{MS}}$ quark mass

The relationship between pole and running $\overline{\text{MS}}$ quark mass is given by [26]

$$m(\mu_m)=M_{\text{pole}}\big[1+a(\mu_a)r_m^{(1)}(\mu_m)+a(\mu_a)^2r_m^{(2)}(\mu_a,\mu_m)+\dots\big]\,, \tag{B.1}$$

where

$$r_m^{(1)}=r_{m,0}^{(1)}-\gamma_1\ln\frac{\mu_m}{m(\mu_m)}\,, \tag{B.2}$$

$$r_m^{(2)}=r_{m,0}^{(2)}-\big[\gamma_2+(\gamma_1-\beta_1)r_{m,0}^{(1)}\big]\ln\frac{\mu_m}{m(\mu_m)}+\frac{\gamma_1}{2}(\gamma_1-\beta_1)\ln^2\frac{\mu_m}{m(\mu_m)}-\left[\gamma_1+\beta_1\ln\frac{\mu_m}{\mu_a}\right]r_m^{(1)}\,. \tag{B.3}$$

The coefficients of the logarithms can be calculated from the renormalization group [43], and the constant coefficients $r_{m,0}^{(1)}$ and $r_{m,0}^{(2)}$ are found to be [44, 45]

$$r_{m,0}^{(1)}=-C_{\mathrm{F}}\,, \tag{B.4}$$

$$\begin{aligned}r_{m,0}^{(2)}=&\,C_{\mathrm{F}}^2\left[\frac{7}{128}-\frac{15}{8}\zeta(2)-\frac{3}{4}\zeta(3)+3\zeta(2)\ln 2\right]\\&+C_{\mathrm{F}}Tn_f\left[\frac{71}{96}+\frac{1}{2}\zeta(2)\right]\\&+C_AC_{\mathrm{F}}\left[-\frac{1111}{384}+\frac{1}{2}\zeta(2)+\frac{3}{8}\zeta(3)-\frac{3}{2}\zeta(2)\ln 2\right]\\&+C_{\mathrm{F}}T\left[\frac{3}{4}-\frac{3}{2}\zeta(2)\right]\,,\end{aligned} \tag{B.5}$$

with

$$\begin{aligned}\beta_1&=\frac{1}{6}[11C_A-4Tn_f]\,,\\ \beta_2&=\frac{1}{12}\big[17C_A^2-10C_ATn_f-6C_{\mathrm{F}}Tn_f\big]\end{aligned} \tag{B.6}$$

and

$$\gamma_1=\frac{3}{2}C_{\mathrm{F}}\,,\quad \gamma_2=\frac{C_{\mathrm{F}}}{48}[97C_A+9C_{\mathrm{F}}-20Tn_f]\,. \tag{B.7}$$

Appendix C: Relevant expressions in the DK continuum contribution

For convenience, in this appendix we collect some relevant expressions used in Sect. 3 when discussing the DK continuum contribution. Firstly, we define the following loop-integral functions $\Sigma_i(t)$ (with $t=q^2$)

$$\begin{aligned}\Sigma_0(t)&=2\mathrm{i}\int\frac{\mathrm{d}^4k}{(2\pi)^4}\frac{1}{\left(k^2-m_K^2\right)\left[(q-k)^2-m_D^2\right]}\\&=-\frac{1}{8\pi^2}B_0\left(t,m_D^2,m_K^2\right)\,,\end{aligned} \tag{C.1}$$

$$\begin{aligned}\Sigma_1(t)&=2\mathrm{i}\int\frac{\mathrm{d}^4k}{(2\pi)^4}\frac{k_0}{\left(k^2-m_K^2\right)\left[(q-k)^2-m_D^2\right]}\\&=-\frac{1}{8\pi^2}\left\{\frac{t+m_K^2-m_D^2}{2\sqrt{t}}B_0\left(t,m_D^2,m_K^2\right)+\frac{1}{2\sqrt{t}}\left[A_0\left(m_D^2\right)-A_0\left(m_K^2\right)\right]\right\}\,,\end{aligned} \tag{C.2}$$

$$\begin{aligned}\Sigma_2(t)&=2\mathrm{i}\int\frac{\mathrm{d}^4k}{(2\pi)^4}\frac{k_0^2}{\left(k^2-m_K^2\right)\left[(q-k)^2-m_D^2\right]}\\&=-\frac{1}{8\pi^2}\left\{\frac{\left(t+m_K^2-m_D^2\right)^2}{4t}B_0\left(t,m_D^2,m_K^2\right)+\frac{t+m_K^2-m_D^2}{4t}\left[A_0\left(m_D^2\right)-A_0\left(m_K^2\right)\right]+\frac{1}{2}A_0\left(m_D^2\right)\right\}\,,\end{aligned} \tag{C.3}$$

$$\begin{aligned}\Sigma_3(t)&=2\mathrm{i}\int\frac{\mathrm{d}^4k}{(2\pi)^4}\frac{k^2}{\left(k^2-m_K^2\right)\left[(q-k)^2-m_D^2\right]}\\&=-\frac{1}{8\pi^2}\left[m_K^2B_0\left(t,m_D^2,m_K^2\right)+A_0\left(m_D^2\right)\right]\,,\end{aligned} \tag{C.4}$$

$$\begin{aligned}\Sigma_4(t)&=2\mathrm{i}\int\frac{\mathrm{d}^4k}{(2\pi)^4}\frac{k^2k_0}{\left(k^2-m_K^2\right)\left[(q-k)^2-m_D^2\right]}\\&=-\frac{1}{8\pi^2}\left\{\frac{t+m_K^2-m_D^2}{2\sqrt{t}}m_K^2B_0\left(t,m_D^2,m_K^2\right)+\frac{m_K^2}{2\sqrt{t}}\left[A_0\left(m_D^2\right)-A_0\left(m_K^2\right)\right]+\sqrt{t}A_0\left(m_D^2\right)\right\}\,,\end{aligned} \tag{C.5}$$

$$\Sigma_5(t)=2\mathrm{i}\int\frac{\mathrm{d}^4k}{(2\pi)^4}\frac{(k^2)^2}{\left(k^2-m_K^2\right)\left[(q-k)^2-m_D^2\right]}$$

$$= -\frac{1}{8\pi^2}\left[m_K^4 B_0(t, m_D^2, m_K^2) + (t + m_K^2 + m_D^2) A_0(m_D^2)\right]. \quad \text{(C.6)}$$

Here we have taken into account two intermediate states with different charges in (C.1)–(C.6). $A_0(m^2)$ and $B_0(t, m_1^2, m_2^2)$ is the usual one-loop scalar one- and two-point function, respectively [46]

$$A_0(m^2) = -\mathrm{i}\int \frac{\mathrm{d}^4 k}{\pi^2}\frac{1}{(k^2 - m^2)} = m^2\left[\left(\frac{2}{\epsilon} - \gamma_{\mathrm{E}} + \ln 4\pi\right) + 1 - \ln\frac{m^2}{\mu^2}\right], \quad \text{(C.7)}$$

$$B_0(t, m_1^2, m_2^2) = -\mathrm{i}\int \frac{\mathrm{d}^4 k}{\pi^2}\frac{1}{(k^2 - m_1^2)\left[(q^2 - k)^2 - m_2^2\right]} = \left(\frac{2}{\epsilon} - \gamma_{\mathrm{E}} + \ln 4\pi\right) + \ln\mu^2 - F_0(t, m_1^2, m_2^2), \quad \text{(C.8)}$$

where $\epsilon = 4 - D$ in D-dimensional space time, μ is the renormalization scale introduced in dimensional regularization, and the explicit form of the function $F_0(t, m_1^2, m_2^2)$ could be found in [47].

From the three linear equations for the three unknown functions $f_i(t)$ given by (13)–(15), we can deduce explicit expressions for the three unknown functions $f_i(t)$:

$$f_0(t) = \frac{1}{Y(t)} 4 f_K^4 g_0\left[\Sigma_0 f_K^2 + \Sigma_1^2 - \Sigma_0\Sigma_2\right](t - t_0), \quad \text{(C.9)}$$

$$f_1(t) = \frac{1}{Y(t)} 2 f_K^4 g_0\left[2\Sigma_1 f_K^2 - \Sigma_1\Sigma_3 + \Sigma_0\Sigma_4 + 2(\Sigma_1^2 - \Sigma_0\Sigma_2)\sqrt{t}\right](t - t_0), \quad \text{(C.10)}$$

$$f_2(t) = \frac{1}{Y(t)} 2 f_K^2 g_0\Big\{2\Sigma_3 f_K^4 + \big[2\Sigma_1\Sigma_4 - \Sigma_3(2\Sigma_2 + \Sigma_3) + \Sigma_0\Sigma_5 + 2(\Sigma_1\Sigma_3 - \Sigma_0\Sigma_4)\sqrt{t}\big] f_K^2 + \Sigma_0\Sigma_4^2 - 2\Sigma_1\Sigma_3\Sigma_4 + \Sigma_1^2\Sigma_5 + \Sigma_2(\Sigma_3^2 - \Sigma_0\Sigma_5)\Big\}(t - t_0), \quad \text{(C.11)}$$

with

$$\begin{aligned} Y(t) = \Big\{&4(\Sigma_0 g_0^2 + M_0^2 - t) f_K^6 + 4\big[(\Sigma_1^2 - \Sigma_0\Sigma_2) g_0^2 + (\Sigma_2 + \Sigma_3 - 2\Sigma_1\sqrt{t})(t - M_0^2)\big] f_K^4 \\ &+ (M_0^2 - t)\big[4t\Sigma_1^2 - 4\Sigma_4\Sigma_1 + \Sigma_3^2 - \Sigma_0\Sigma_5 + 4\Sigma_2(\Sigma_3 - \Sigma_0 t) - 4(\Sigma_1\Sigma_3 - \Sigma_0\Sigma_4)\sqrt{t}\big] f_K^2 \\ &+ \big[2\Sigma_3\Sigma_4\Sigma_1 - \Sigma_5\Sigma_1^2 - \Sigma_0\Sigma_4^2 - \Sigma_2(\Sigma_3^2 - \Sigma_0\Sigma_5)\big] \times (M_0^2 - t)\Big\}(t - t_0) \\ &- 4 c f_K^4 g_0^2(\Sigma_0 f_K^2 + \Sigma_1^2 - \Sigma_0\Sigma_2)(M_0^2 - t). \end{aligned} \quad \text{(C.12)}$$

With the above results, the functions $\Delta(t)$ and $\Delta_1(t)$ can respectively be written as

$$\begin{aligned} \Delta(t) &= \frac{(3t - m_D^2 + m_K^2)(M_0^2 - t)}{32 f_K^2\pi^2 t} A_0(m_D^2) + \frac{(3t - m_K^2 + m_D^2)(M_0^2 - t)}{32 f_K^2\pi^2 t} A_0(m_K^2) \\ &+ \frac{c f_K^2 g_0^2(t - M_0^2) + \big(f_K^2 g_0^2 - (t - M_0^2)(t - m_D^2)\big)(t - t_0)}{256 f_K^4\pi^4 t(t - t_0)} \times A_0(m_D^2)^2 \\ &+ \frac{c f_K^2 g_0^2(t - M_0^2) + \big(f_K^2 g_0^2 - (t - M_0^2)(t - m_K^2)\big)(t - t_0)}{256 f_K^4\pi^4 t(t - t_0)} \\ &\times A_0(m_K^2)^2 - \big\{2 c f_K^2 g_0^2(t - M_0^2) + \big(2 f_K^2 g_0^2 + (t - M_0^2)(t + m_D^2 + m_K^2)\big)(t - t_0)\big\} \\ &\times \frac{1}{256 f_K^4\pi^4 t(t - t_0)} \times A_0(m_D^2) A_0(m_K^2) \\ &- \frac{(t - m_D^2 + m_K^2) A_0(m_D^2) + (t - m_K^2 + m_D^2) A_0(m_K^2)}{8192 f_K^6\pi^6 t} \times (t - M_0^2) A_0(m_D^2) A_0(m_K^2) \\ &- \frac{g_0^2}{8\pi^2} B_0(t, m_D^2, m_K^2) - \frac{c g_0^2(t - M_0^2)}{8\pi^2(t - t_0)} B_0(t, m_D^2, m_K^2) \\ &- \frac{(t - M_0^2)\big((m_D^2 - m_K^2)^2 + 2(m_D^2 + m_K^2)t - 3t^2\big)}{32 f_K^2\pi^2 t} \times B_0(t, m_D^2, m_K^2) \\ &- \frac{\left\{\begin{array}{l}(t + m_D^2 - m_K^2)\big(c f_K^2 g_0^2(t - M_0^2) \\ + \big(f_K^2 g_0^2 - (t - M_0^2)(t - m_D^2)\big)(t - t_0)\big)\end{array}\right\}}{256 f_K^4\pi^4 t(t - t_0)} \times A_0(m_D^2) B_0(t, m_D^2, m_K^2) \\ &- \frac{\left\{\begin{array}{l}(t + m_K^2 - m_D^2)\big(c f_K^2 g_0^2(t - M_0^2) \\ + \big(f_K^2 g_0^2 - (t - M_0^2)(t - m_K^2)\big)(t - t_0)\big)\end{array}\right\}}{256 f_K^4\pi^4 t(t - t_0)} \times A_0(m_K^2) B_0(t, m_D^2, m_K^2) \\ &+ \frac{\big(t^2 - (m_D^2 - m_K^2)^2\big)(t - M_0^2)}{8192 f_K^6\pi^6 t} \times A_0(m_D^2) A_0(m_K^2) B_0(t, m_D^2, m_K^2). \end{aligned} \quad \text{(C.13)}$$

$$\Delta_1(t) = N(t)/D(t), \quad \text{(C.14)}$$

$$\begin{aligned} N(t) = {}& 32 f_K^4 g_0^2\pi^2(t - t_0)\left[A_0(m_K^2)^2 + A_0(m_D^2)^2\right] - 64 f_K^4 g_0^2\pi^2(t - t_0) A_0(m_K^2) A_0(m_D^2) \\ &- 32 f_K^4 g_0^2\pi^2(t - t_0)\big[(m_D^2 - m_K^2 + t) A_0(m_D^2) - (m_D^2 - m_K^2 - t) A_0(m_K^2)\big] B_0(t, m_D^2, m_K^2) \\ &- 1024 f_K^6 g_0^2\pi^4 t(t - t_0) B_0(t, m_D^2, m_K^2), \end{aligned} \quad \text{(C.15)}$$

$$\begin{aligned} D(t) = {}& 256 f_K^4\pi^4(t - t_0)\big[(3t - m_D^2 + m_K^2) A_0(m_D^2) + (3t + m_D^2 - m_K^2) A_0(m_K^2)\big] \\ &+ (t - t_0)\big[(t - m_D^2 + m_K^2) A_0(m_D^2) + (t + m_D^2 - m_K^2) A_0(m_K^2)\big] A_0(m_D^2) A_0(m_K^2) \\ &+ 32 f_K^2\pi^2\big[2 c f_K^2 g_0^2 + (m_D^2 + m_K^2 + t)(t - t_0)\big] \times A_0(m_D^2) A_0(m_K^2) \\ &- 32 f_K^2\pi^2\big\{\big[c f_K^2 g_0^2 + (m_D^2 - t)(t - t_0)\big] A_0(m_D^2)^2 + \big[c f_K^2 g_0^2 + (m_K^2 - t)(t - t_0)\big] A_0(m_K^2)^2\big\} \end{aligned}$$

$$
\begin{aligned}
&+\left[\left(m_D^2-m_K^2\right)^2-t^2\right](t-t_0)\\
&\times A_0\left(m_D^2\right)A_0\left(m_K^2\right)B_0\left(t,m_D^2,m_K^2\right)\\
&+32f_K^2\pi^2\left\{\left(m_D^2-m_K^2+t\right)\right.\\
&\times\left[cf_K^2g_0^2+\left(m_D^2-t\right)(t-t_0)\right]A_0\left(m_D^2\right)\\
&-\left(m_D^2-m_K^2-t\right)\left[cf_K^2g_0^2+\left(m_K^2-t\right)(t-t_0)\right]\\
&\left.\times A_0\left(m_K^2\right)\right\}B_0\left(t,m_D^2,m_K^2\right)\\
&+256f_K^4\pi^4\left\{4cf_K^2g_0^2t+\left[\left(m_D^2-m_K^2\right)^2\right.\right.\\
&\left.\left.+2\left(m_D^2+m_K^2\right)t-3t^2\right](t-t_0)\right\}B_0\left(t,m_D^2,m_K^2\right)\\
&+8192f_K^6\pi^6t(t-t_0)\,. \qquad \text{(C.16)}
\end{aligned}
$$

References

1. BABAR Collaboration, B. Aubert et al., Phys. Rev. Lett. **90**, 242 001 (2003)
2. CLEO Collaboration, D. Besson et al., AIP Conf. Proc. **698**, 497 (2004)
3. S. Godfrey, R. Kokoski, Phys. Rev. D **43**, 1679 (1991)
4. S. Godfrey, N. Isgur, Phys. Rev. D **32**, 189 (1985)
5. M. Di Pierro, E. Eichten, Phys. Rev. D **64**, 114 004 (2001)
6. Y.-B. Dai, C.-S. Huang, H.-Y. Jin, Phys. Lett. B **331**, 174 (1994)
7. E. van Beveren, G. Rupp, Phys. Rev. Lett. **91**, 012 003 (2003)
8. E. van Beveren, G. Rupp, Eur. Phys. J. C **32**, 493 (2004)
9. G.S. Bali, Phys. Rev. D **68**, 071 501 (2003)
10. A. Dougall, R.D. Kenway, C.M. Maynard, C. McNeile, Phys. Lett. B **569**, 41 (2003)
11. H.W. Lin, S. Ohta, A. Soni, N. Yamada, Phys. Rev. D **74**, 114 506 (2006)
12. H.-Y. Cheng, W.-S. Hou, Phys. Lett. B **566**, 193 (2003)
13. T. Barnes, F.E. Close, H.J. Lipkin, Phys. Rev. D **68**, 054 006 (2003)
14. A.P. Szczepaniak, Phys. Lett. B **567**, 23 (2003)
15. J. Vijande, F. Fernandez, A. Valcarce, Phys. Rev. D **73**, 034 002 (2006)
16. H.X. Zhang, W.L. Wang, Y.B. Dai, Z.Y. Zhang, hep-ph/0607207
17. P. Colangelo, F. De Fazio, A. Ozpineci, Phys. Rev. D **72**, 074 004 (2005)
18. BABAR Collaboration, B. Aubert, Phys. Rev. Lett. **97**, 222 001 (2006)
19. Y.-B. Dai, C.-S. Huang, C. Liu, S.-L. Zhu, Phys. Rev. D **68**, 114 011 (2003)
20. P. Colangelo, G. Nardulli, A.A. Ovchinnikov, N. Paver, Phys. Lett. B **269**, 201 (1991)
21. A. Hayashigaki, K. Terasaki, hep-ph/0411285
22. S. Narison, Phys. Lett. B **605**, 318 (2005)
23. K.G. Chetyrkin, M. Steinhauser, Phys. Lett. B **502**, 104 (2001) [arXiv:hep-ph/0012002]
24. K.G. Chetyrkin, M. Steinhauser, Eur. Phys. J. C **21**, 319 (2001) [arXiv:hep-ph/0108017]
25. W.A. Bardeen, A.J. Buras, D.W. Duke, T. Muta, Phys. Rev. D **18**, 3998 (1978)
26. M. Jamin, B.O. Lange, Phys. Rev. D **65**, 056 005 (2002) [arXiv:hep-ph/0108135]
27. P. Colangelo, F. De Fazio, G. Nardulli, N. Di Bartolomeo, R. Gatto, Phys. Rev. D **52**, 6422 (1995)
28. S.-L. Zhu, Y.-B. Dai, Mod. Phys. Lett. A **14**, 2367 (1999)
29. B. Blok, M. Shifman, N. Uraltsev, Nucl. Phys. B **494**, 247 (1997)
30. G. t'Hooft, Nucl. Phys. B **61**, 455 (1973)
31. J.H. Kuhn, M. Steinhauser, C. Sturm, Nucl. Phys. B **778**, 192 (2007)
32. S. Bethke, Prog. Part. Nucl. Phys. **58**, 351 (2007)
33. S. Narison, Phys. Rev. D **74**, 034 013 (2006)
34. Particle Data Group, W.M. Yao et al., J. Phys. G **33**, 1 (2006)
35. J. Bordes, J. Penarrocha, K. Schilcher, JHEP **0511**, 014 (2005) [arXiv:hep-ph/0507241]
36. J. Bordes, J. Penarrocha, K. Schilcher, JHEP **0412**, 064 (2004) [arXiv:hep-ph/0410328]
37. M. Jamin, M. Munz, Z. Phys. C **60**, 569 (1993) [arXiv:hep-ph/9208201]
38. D.J. Broadhurst, Phys. Lett. B **101**, 423 (1981)
39. S.C. Generalis, J. Phys. G **16**, 785 (1990)
40. V.P. Spiridonov, K.G. Chetyrkin, Sov. J. Nucl. Phys. **47**, 522 (1988)
41. V.P. Spiridonov, K.G. Chetyrkin, Yad. Fiz. **47**, 818 (1988)
42. K.G. Chetyrkin, C.A. Dominguez, D. Pirjol, K. Schilcher, Phys. Rev. D **51**, 5090 (1995)
43. K.G. Chetyrkin, J.H. Kuhn, M. Steinhauser, Nucl. Phys. B **482**, 213 (1996)
44. R. Tarrach, Nucl. Phys. B **183**, 384 (1981)
45. N. Gray, D.J. Broadhurst, W. Grafe, K. Schilcher, Z. Phys. C **48**, 673 (1990)
46. G. Passarino, M.J.G. Veltman, Nucl. Phys. B **160**, 151 (1979)
47. M. Drees, based on a talk given at 2nd Workshop on High Energy Physics Phenomenology, Calcutta, India, Jan 2–15, 1991